Review

Review of constituent retrieval in optically deep and complex waters from satellite imagery

Daniel Odermatt [a,*], Anatoly Gitelson [b], Vittorio Ernesto Brando [c], Michael Schaepman [a]

[a] Remote Sensing Laboratories, University of Zurich, Switzerland
[b] School of Natural Resources, University of Nebraska, Lincoln, Nebraska, United States
[c] CSIRO Land and Water, Environmental Earth Observation Programme, Canberra, Australian Capital Territory 2601, Australia

ARTICLE INFO

ABSTRACT

We provide a comprehensive overview of water constituent retrieval algorithms and underlying definitions and models for optically deep and complex (i.e. case 2) waters using earth observation data. The performance of constituent retrieval algorithms is assessed based on matchup validation experiments published between January 2006 and May 2011. Validation practices range from singular vicarious calibration experiments to comparisons using extensive in situ time series. Band arithmetic and spectral inversion algorithms for all water types are classified using a method based scheme that supports the interpretation of algorithm validity ranges. Based on these ranges we discuss groups of similar algorithms in view of their strengths and weaknesses. Such quantitative literature analysis reveals clear application boundaries. With regard to chlorophyll retrieval, validation of blue–green band ratios in coastal waters is limited to oligotrophic, predominantly ocean waters, while red-NIR ratios apply only at more than 10 mg/m^3. Spectral inversion techniques — although not validated to the same extent — are necessary to cover all other conditions. Suspended matter retrieval is the least critical, as long as the wavelengths used in empirical models are increased with concentrations. The retrieval of dissolved organic matter however remains relatively inaccurate and inconsistent, with large differences in the accuracy of comparable methods in similar validation experiments. We conclude that substantial progress has been made in understanding and improving retrieval of constituents in optically deep and complex waters, enabling specific solutions to almost any type of optically complex water. Further validation and intercomparison of spectral inversion procedures are however needed to learn if solutions with a larger validity range are feasible.

© 2011 Elsevier Inc. All rights reserved.

Contents

1. Introduction

Optically deep and complex waters are referred to as case 2 waters, as opposed to phytoplankton dominated case 1 waters of the open

* Corresponding author. Tel.: +41 446356517; fax: +41 446356846.
 E-mail address: daniel.odermatt@geo.uzh.ch (D. Odermatt).

ocean (Morel & Prieur, 1977). The variety within case 2 waters is large, because concentrations as well as specific inherent optical properties of chlorophyll (CHL), total suspended matter (TSM) and colored dissolved organic matter concentrations (CDOM) are subject to potentially large and independent variations. Satellite sensors such as SeaWiFS, MODIS, and MERIS are currently being used to deliver ocean color data, attaining the requirements necessary for ocean biogeochemistry and climate research (Dierssen, 2010; McClain, 2009). Alas, universally applicable algorithms for the retrieval of water constituents from case 2 waters are not known (IOCCG, 2006, 2009). Specific algorithms are thus optimized and validated for commonly understood but ill-defined water types, e.g. turbid (Gitelson et al., 2007) or clear water (Belzile et al., 2004). Other authors address trophic classes (Cheng Feng et al., 2009; Dekker & Peters, 1993; Iluz et al., 2003), for which several diverging definitions exist (Bukata et al., 1995; Carlson & Simpson, 1996; Chapra & Dobson, 1981; Nürnberg, 1996; Wetzel, 1983). Trophic thresholds vary however with ecosystem specific limitations to primary productivity, while the validity of remote sensing algorithms is determined only by the variability in optical properties.

Carder et al. (1999) and Morel (1980) distinguish empirical and analytical methods for water constituent retrieval, and in-betweens with the epithet "semi-". Empirical algorithms are derived by statistical regression (Kabbara et al., 2008; Mahasandana et al., 2009) or endmember selection (Tyler et al., 2006), which implies effective data optimization but limited transferability (Austin & Petzold, 1981). Analytical algorithms are based on simplified solutions of the radiative transfer equation. This usually requires approximations or calibration with empirical coefficients (Carder et al., 1999), while statistical regression often leads to solutions that coincide with properties known from physical models (e.g. normalizing band ratios (Gitelson, 1992)), explaining the epithet "semi-" from either side. Either type of algorithm is usually applied as a band arithmetic solution for one constituent at a time, although empirical solutions can also be found by other approaches (Gonzalez Vilas et al., 2011; Tyler et al., 2006).

In contrast, spectral inversion procedures match spectral measurements with bio-optical forward models by means of inversion techniques. The spectral inherent optical properties (IOPs, (Preisendorfer, 1961)) of all three constituents are thereby retrieved at once from one spectral apparent property (AOP). Several inversion techniques are applied for this procedure, whereby the investigated AOP is matched with simulated AOPs from bio-optical forward models, i.e. either analytical relationships (Albert & Mobley, 2003; Gordon et al., 1975; Lee et al., 2002; Maritorena et al., 2002; Park & Ruddick, 2005) or numerical radiative transfer models (Bulgarelli et al., 1999; Jin & Stamnes, 1994; Mobley, 1989; Zhai et al., 2010).

By comprehensively reviewing the literature from 2006 to May 2011, we discuss in this paper recent studies reporting matchup validation results for water constituent retrieval in case 2 waters from satellite imagery using band ratio or spectral inversion algorithms. Accuracy assessments for band ratio or spectral inversion algorithms based only on in situ measurements, e.g. Kostadinov et al. (2007)), Moore et al. (2009) or Shanmugam et al. (2010) or simulated datasets, e.g. Qin et al. (2007) are not discussed. This work complements the review of the accomplishments in ocean color research in the last decade by McClain (2009), as well as the exhaustive review of empirical algorithms for case 2 waters (Matthews, 2011) extending earlier work by Dekker et al. (1995).

We group the paper in 7 sections, where the relevance of IOPs and AOPs in models and algorithms is discussed first, followed by a description of band arithmetic and spectral inversion algorithms. Recent validation experiments for either approach are then summarized and quantitatively analyzed for their range of applicability.

2. Relevance of IOPs in models and algorithms

Regarding IOPs, the volume scattering function $\beta(\psi)$ is the elementary property for the integration of the scattering and backscattering coefficients b and b_b, respectively, over scattering angle ψ. Measurements of $\beta(\psi)$ (Chami et al., 2006; Freda & Piskozub, 2007; Freda et al., 2007; Lee & Lewis, 2003; Petzold, 1972; Sokolov et al., 2010; Sullivan & Twardowski, 2009) are normalized to the scattering phase function $\tilde{\beta}(\psi)$. Several models of $\tilde{\beta}(\psi)$ have been proposed to approximate these measurements (Fournier & Forand, 1994; Fournier & Jonasz, 1999; Haltrin, 2002; Mobley et al., 1993). Their effect on calculated reflectance quantities is up to 20% (Chami et al., 2006; Gordon, 1993; Mobley et al., 2002; Morel & Gentili, 1996; Morel et al., 2002). The ratio of molecular to total scattering, η, is a major proxy for the shape of $\beta(\psi)$, since molecular $\tilde{\beta}_W$ is less anisotropic than particulate $\tilde{\beta}_{TSM}$ (Morel, 1974; Smith & Baker, 1981).

The absorption coefficient a in contrast is omnidirectional, but influences the intensity and anisotropy of reflectance through the single scattering albedo ω_0 (Gordon & Brown, 1973; Gordon et al., 1975; Morel & Prieur, 1977) and the number of subsequent scattering events of a photon before reaching the interface, N (Loisel & Morel, 2001; Morel et al., 2002), respectively. An alternative term for the former is the single backscattering albedo ω_b. The latter indicates the blurring of $\beta(\psi)$ in turbid water (Pfeiffer & Chapman, 2008; Piskozub & McKee, 2011; Sydor, 2007).

The ability to account for variations in these IOPs is limited for band arithmetic algorithms, while increasingly addressed by spectral inversion algorithms for radiative transfer simulations (Doerffer & Schiller, 2007; Schroeder et al., 2007b; Van Der Woerd & Pasterkamp, 2008) or specific semi-analytical models (Albert & Mobley, 2003; Park & Ruddick, 2005).

3. Relevance of AOPs in models and algorithms

The first widely used AOP is the bihemispherical irradiance reflectance R^-, which is related to ω_b in the earliest semi-analytical models for case 2 water by means of the linear coefficient f (Gordon et al., 1975; Morel & Prieur, 1977), which again varies with illumination zenith angle θ_s^+ (Gordon, 1989; Kirk, 1991; Sathyendranath & Platt, 1997).

Subsequent experiments for case 1 (Morel & Gentili, 1991, 1993) and case 2 (Loisel & Morel, 2001) waters focus on anisotropy of the underwater light field, described by η, N and the anisotropy factor Q that relates diffuse upwelling irradiance E_u^- to directional upwelling radiance L_u^-. It is found that the directional variations in f and Q partly compensate each other, leaving the subsurface remote sensing reflectance R_{rs}^- less sensitive to anisotropy effects than R^- (Morel & Gentili, 1993). Accordingly, semi-analytical models that relate ω_b directly to R_{rs}^- by means of quadratic coefficients became more popular (Gordon et al., 1988; Lee et al., 1998).

Correction for air–water interface and normalization of the resulting R_{rs}^+ to zenith illumination and viewing geometry will then result in the normalized water-leaving reflectance $[R_w]_N$ (Gordon & Clark, 1981; Gordon et al., 1988). The calculation of $[R_w]_N$ from at-sensor radiances as well as estimation of the coefficients in semi-analytical models requires knowledge of atmospheric and aquatic parameters, which have to be retrieved through iterative procedures (Gordon & Franz, 2008; Morel & Gentili, 1996). Since such procedures are more computationally expensive for case 2 than for case 1 waters (Kuchinke et al., 2009a), approximations find wide use in both cases, compromising the potential improvement due to such normalizations.

4. Band arithmetic algorithms

CHL retrieval band arithmetic algorithms make use of the pigment's primary and secondary absorption maxima at 442 nm and 665 nm, respectively (Bricaud et al., 1995), a reflectance peak around 700 nm due to the minimum sum of absorption of phytoplankton, particulate and dissolved matter and water (Gitelson, 1992; Vasilkov &

Kopelevich, 1982; Vos et al., 1986) and its fluorescence emission band at 681 nm (Gower et al., 1999).

The primary feature is superimposed by CDOM absorption (Bricaud et al., 1981), and therefore widely used in case 1 waters, where CDOM and CHL correlate as CDOM is a phytoplankton degradation product (Morel & Prieur, 1977). Sensor specific standard algorithms for primary CHL absorption bands exist for all medium resolution ocean color spectrometers (Aiken et al., 1995; Clark, 1997; Morel & Antoine, 2007; Murakami et al., 2006; O'Reilly et al., 1998). They are referred to as OC2, OC3 and OC4 depending on the number of bands used.

Using the secondary feature is promoted by weak variations in the spectral properties of all other parameters apart from the increasing absorption by water (Dall'Olmo et al., 2003; Gitelson, 1992; Schalles et al., 1998). Its major limitation is the absence of the feature in oligotrophic and some mesotrophic lakes (Guanter et al., 2010).

Fluorescence line height (FLH) and maximum chlorophyll index (MCI) algorithms are linear baseline algorithms for <30 mg/m^3 and >100 mg/m^3 CHL ranges (Gower et al., 2005). They can be applied either with or without atmospheric correction (Binding et al., 2011; Matthews et al., 2010).

TSM and corresponding particle scattering is best quantified outside the CHL or CDOM features (Binding et al., 2010). Regression with a single band is possible if an accurate, possibly NIR L_w coupled atmospheric correction is applied (Stumpf et al., 2003). Multi band algorithms are however also used on uncorrected at-sensor radiances (Koponen et al., 2007). The choice of spectral bands in regression algorithms depends on the corresponding concentrations ranges, whereas appropriate wavelengths shift from 550 nm towards the red and NIR portions of the spectral range for increasing TSM (Wang & Lu, 2010). The increase in absorption of pure water towards the NIR will namely require increasing TSM to ensure a sufficient reflectance signal (Ruddick et al., 2006), while less absorbing portions of the spectrum are more suitable for low concentrations. Empirical regression of in situ TSM with all eligible bands of a spectroradiometric measurement is a simple way to test this hypothesis (Nechad et al., 2010), and provides the flexibility to derive suitable algorithms even for Landsat TM instruments (Wang et al., 2009; Zhou et al., 2006).

CDOM retrieval methods are restricted to short visible wavelengths, where absorptions of CDOM and CHL coincide (Babin et al., 2003; Ferreira et al., 2009) and inaccuracies due to NIR derived atmospheric correction are largest (Hu et al., 2000). Accordingly, most band arithmetic approaches relate CDOM to a ratio of sensitive bands at <600 nm and normalization bands at >600 nm (Kallio et al., 2001).

The choice of suitable sensors is smaller than for the estimation of CHL and TSM, due to insufficient radiometric accuracy of Hyperion (Giardino et al., 2007) and Landsat Thematic Mapper (Kutser et al., 2005b) in the short wave domain of the spectrum.

5. Spectral inversion algorithms

The constitution of spectral inversion algorithms is more heterogeneous than band arithmetic algorithms, with differences in water, interface, atmospheric models and inversion techniques. Spectral inversion algorithms perform a simultaneous retrieval of IOPs and concentrations of the optically active constituents. One of the major weaknesses of these algorithms is related to the appropriate parameterization of the IOP spectral shapes (IOCCG, 2006).

Table 1 contains a list of recent studies reporting validation results for spectral inversion algorithms in case 2 waters. NN inversion techniques are dominant, probably due to their improved availability as MERIS level 2 products (Doerffer & Schiller, 2007) and by BEAM plug-ins (Doerffer & Schiller, 2008a; Schroeder et al., 2007b). Other inversion techniques include area minimization (Kutser et al., 2001), matrix inversion (Brando & Dekker, 2003), downhill simplex (Heege & Fischer, 2004), least-squares (Santini et al., 2010), spectral optimization (Kuchinke et al., 2009a) and Levenberg–Marquardt optimization (Van Der Woerd & Pasterkamp, 2008). Only one application of the SeaDAS semi-analytical algorithms (Carder et al., 1999; Lee et al., 2002; Maritorena et al., 2002) is listed in Table 1. This is however to a large extent due to their focus on retrieving IOPs rather than constituent concentrations.

Most algorithms are used together with specific atmospheric correction modules. The use of standard level 2 reflectance products is only foreseen for two algorithms (Schuchman et al., 2005; Van Der Woerd & Pasterkamp, 2008). The inversion modules match atmospherically corrected R_{rs}^+ or R^- with Hydrolight simulated data (Brando & Dekker, 2003; Doerffer & Schiller, 2007, 2008a; Santini et al., 2010; Van Der Woerd & Pasterkamp, 2008), other numerical (Jerome et al., 1996; Pozdnyakov et al., 2005) or semi-analytical (Heege & Fischer, 2004; Kuchinke et al., 2009a) simulations. Findings from the validation experiments in Table 1 are discussed later.

6. Validation experiments

Recent ISI journals (2006–2011) comprise about 50 published papers reporting water constituent retrieval from satellite imagery for

Table 1

List of matchup validation experiments with spectral inversion processed spaceborne data. Concentration thresholds in bold letters indicate successful quantitative validation, italic letters indicate successful quantitative falsification, and regular letters indicate missing validation. Expected minimum R^2 for validation is 0.4 (CHL, CDOM, tripton) and 0.6 (TSM). Asterisks (*) indicate retrieval of tripton instead of TSM; circles (°) indicate retrieval of inorganic suspended matter instead of TSM; plus signs ($^+$) indicate "dissolved organics" [mgC/l] instead of CDOM; carets (^) indicate "colored detrital matter" [m^{-1}] instead of CDOM. Concentrations in absorption units are given at 400 nm and, if originally given in another wavelength, converted according to Smith and Baker (1981) with explicitly given spectral exponents (Matthews et al., 2010; Santini et al., 2010) or an approximate 0.017 spectral exponent where not specified (Binding et al., 2011; Giardino et al., 2010; Schroeder et al., 2007b; Van Der Woerd & Pasterkamp, 2008). Algorithm references: [1]Doerffer and Schiller (2007), Moore et al. (1999); [2]Doerffer and Schiller (2008a, 2008b); [3]Schroeder et al. (2007a, 2007b); [4]Pozdnyakov et al. (2005); [5]Brando and Dekker (2003); [6]Heege and Fischer (2004). Strict and relaxed matchups chosen from Cui et al. (2010), Kuchinke et al. (2009b) is omitted due to a lack of absolute in situ concentration values.

Experiment	Algorithm	CHL [mg/m^3]		TSM [g/m^3]		CDOM [m^{-1}]	
		max	min	max	min	max	min
Binding et al. (2011)	NN algal_2[1]	70.5	1.9	19.6	0.8	7.1	0.5
Cui et al. (2010)	NN algal_2[1]	16.1	0.7	67.8	1.5	2.0	0.7
Minghelli-Roman et al. (2011)	NN algal_2[1]	9.0	0.0	–	–	–	–
Binding et al. (2011)	NN C2R[2]	70.5	1.9	19.6	0.8	7.1	0.5
Giardino et al. (2010)	NN C2R[2]	74.5	11.67	–	–	4.0	1.3
Matthews et al. (2010)	NN C2R[2]	247.4	69.2	60.7	30.0	7.1	3.4
Odermatt et al. (2010)	NN C2R[2]	9.0	0.0	–	–	–	–
Schroeder et al. (2007b)	NN FUB[3]	12.6	0.1	14.3	2.7	2.0	0.8
Shuchman et al. (2006)	Coupled NN[4]	2.5	0.1	2.7°	1.3°	3.5$^+$	0.0$^+$
Giardino et al. (2007)	MIM[5]	2.2	1.3	2.1*	0.9*	–	–
Odermatt et al. (2008)	MIP[6]	4.0	0.6	–	–	–	–
Santini et al. (2010)	2 step inversion	5.0	1.8	13.0*	3.0*	0.8	0.1
Van der Woerd and Pasterkamp (2008)	Hydropt	20.0	0.0	30.0	0.0	1.6	0.0

optically deep and complex waters, among which about three quarter apply band arithmetic algorithms. Applied selection criteria are the availability of coinciding validation data, concentration ranges and statistical quality measures, namely R^2.

6.1. Chlorophyll-a retrieval

All recent band arithmetic *CHL* retrieval applications are depicted in Fig. 1, with corresponding sensors and concentration ranges. The three previously described major groups are distinguished; green/blue ratios defined for OC algorithms, red-NIR band ratios and further empirical algorithms.

The OC2-OC4 algorithms are successfully applied to retrieve 0–10 mg/m^3 *CHL* in optically complex water. They are however considerably less accurate than red-NIR ratios at high *CHL*, which coincides with theoretical concerns that their use is limited to Open Ocean. This is because independently varying *CDOM* disturb the correlation between such short wavelengths and the primary *CHL* absorption feature. From top to bottom in Fig. 1, study areas are Lake Erie (OC2 and OC4), the Mississippi Delta (OC2), Lake Tanganyika (OC3) and the Northern Adriatic Sea (OC3 and OC4), and a lagoon in New Caledonia (OC4). Several of these examples indicate that the observed water optical properties resemble those in case 1 water to some extent. Mélin et al. (2007) mention that two thirds of their observations refer to case 1 water, and Horion et al. (2010) assume explicitly that even Lake Tanganyika is case 1. The data by D'Sa et al. (2006) follow a shifted but correlated mixture of constituents as found for case 1 water (Morel & Maritorena, 2001), which can be accounted for by regional adjustment as done by Witter et al. (2009). Dupouy et al. (2010) present a turbidity index for the preselection of applicable data points. Atmospheric correction algorithms

provide R_{rs}^+ and $[R_w]_N$ output for the application of the OC algorithms (Gordon & Voss, 2004; Gordon & Wang, 1994; Siegel et al., 2000; Stumpf et al., 2003; Toratani et al., 2007). Further OC applications to optically complex waters lack quantitative matchup validation (Gons et al., 2008; Wang et al., 2011; Werdell et al., 2009).

NIR-red algorithms using 2 or 3 bands are validated using MERIS data for up to 250 mg/m^3 *CHL* in Zeekoevlei (Matthews et al., 2010), and suitable for the 10–100 mg/m^3 interval represented by the Dnieper River, the Sea of Azov, the Gulf of Finland, Lake Dianchi and Kasumigaura, as in vertical order in Fig. 1. *CHL* <10 mg/m^3 is only observed in Moses et al. (2009a; 2009b). Their calibration data and root mean square errors (RMSEs), as well as previous simulations (Dall'Olmo & Gitelson, 2006) indicate a minimum applicability threshold at 10 mg/m^3 *CHL* although lower *CHL* is successfully retrieved from field spectroscopy measurements (Gitelson et al., 2009). Enhancement of NIR-red algorithms by *CDOM* and tripton derived coefficients from a look-up-table may even extend the applicable range, but are only validated for waters with high *CHL* (Yang et al., 2011). Advantages in the use of either 2 or 3 bands are inconsistent (Moses et al., 2009a; Moses et al., 2009b). Larger differences in accuracy occur through different atmospheric correction methods. The MERIS bright pixel procedure (Moore et al., 1999) performs considerably better than the C2R atmosphere module (Doerffer & Schiller, 2008b) in Moses et al. (2009b). Other procedures are SCAPE-M (Guanter et al., 2010) for MERIS (Yang et al., 2011) and FLAASH (Cooley et al., 2002) for Hyperion (Chen et al., 2011), which imply the use of either R_{rs}^+ or R^- for *CHL* retrieval. Matthews et al. (2010) demonstrate that NIR-red algorithms can even be used with uncorrected data at the top of atmosphere (TOA). The same applies to MCI, which outperforms FLH, the MERIS Algal_2 and C2R algorithms at the remote measurement of an algae bloom event in the Lake of
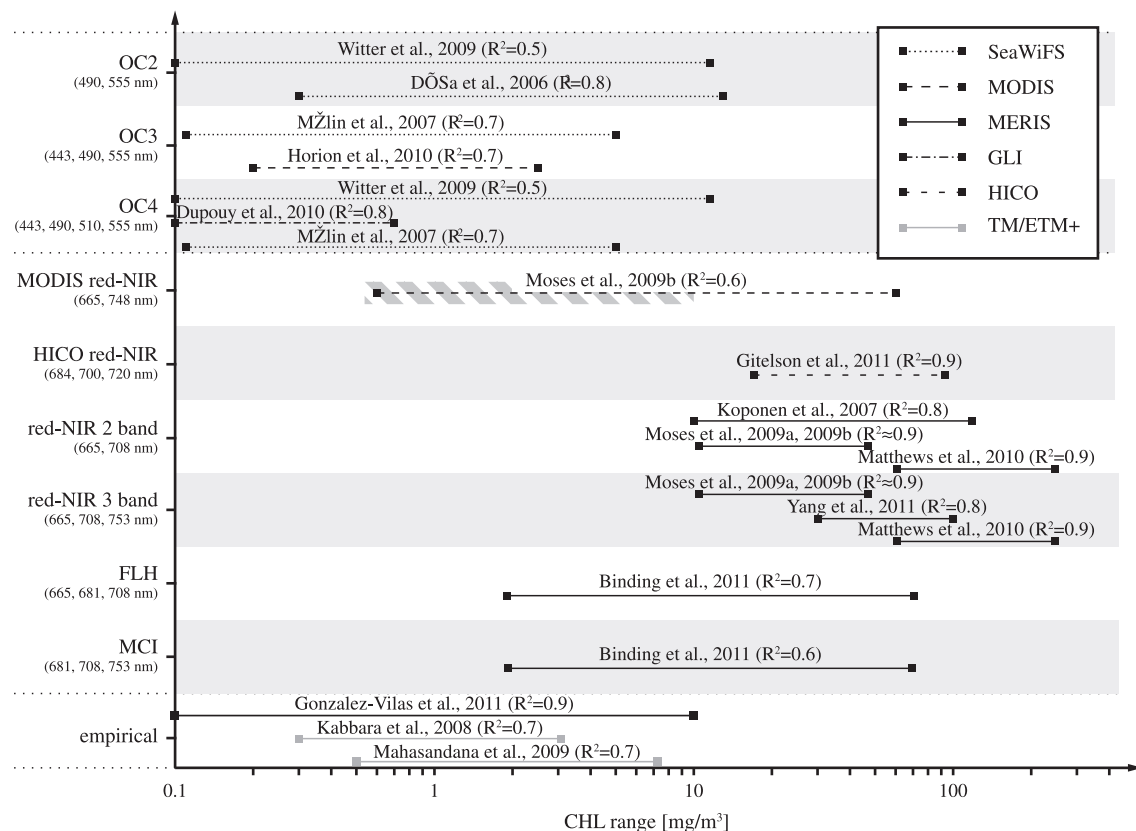
Fig. 1. Overview of recently (2006–2011) published ISI journal papers on the separate retrieval of chl-a from satellite imagery using matchup-validated semi-analytical and empirical algorithms. Hatched areas indicate disputed application ranges. The red-NIR 3 band application by Chen et al. (2011) is omitted since the variation range retrieved from Hyperion (21–27 mg/m^3; $R^2 = 0.6$) is too small to display.

the Woods (Binding et al., 2011). Accuracy restrictions for low *CHL* are however similar as for the 2 and 3 band NIR-red algorithms as far as RMSE (5.7 and 7.3 mg/m³ for MCI and FLH, respectively) is concerned. FLH was also found inapplicable to oligotrophic water in the Laurentian Lakes, raising concerns over the fluorescence signal to noise ratio under unfavourable atmospheric conditions (Gons et al., 2008).

The empirical studies by Kabbara et al. (2008) and Mahasandana et al. (2009) consist of regression models for Landsat-7 ETM+ and Landsat-5 TM. They prove the feasibility of *CHL* estimation with high-resolution sensors, but need parameterization for each single image. In contrast, Gonzalez Vilas et al. (2011) train NNs for preclassified MERIS observations and in situ measured concentrations without the application of an explicit bio-optical model. Their approach achieves high accuracy and temporal stability at the expense of regional restriction.

The types of sensors used in the present experiments correlate clearly with the choice of applications; SeaWiFS and MODIS for the OC algorithms and low *CHL* concentrations, MERIS for the retrieval of high *CHL* by means of red-NIR band ratios and Landsat for empirical algorithms. The advantage of MERIS' 681 nm and 708 nm bands over comparable instruments that lack these bands is known (Gitelson et al., 2008; Gower et al., 1999), and demonstrated for MODIS by Moses et al. (2009a). Gitelson et al. (2011) use a set of hyperspectral HICO data to define optical band positions for a 3 band red-NIR algorithm at even higher accuracy.

Appropriate atmospheric corrections that preserve the NIR reflectance peak and allow for directional normalization to $[R_w]_N$ are another prerequisite and asset, respectively. The SeaDAS toolbox for SeaWiFS and MODIS offers a large variety in this regard (Hu et al., 2000; Ruddick et al., 2000; Stumpf et al., 2003; Vidot & Santer, 2005; Wang, 2007), whereas occasional failure in retrieving the NIR

peak is reported for MERIS' C2R atmospheric correction module (Guanter et al., 2010; Odermatt et al., 2010).

6.2. Suspended sediment retrieval

Recent *TSM* retrieval validation experiments are listed in Fig. 2, for increasing central wavelengths of chosen sensors and bands in vertical direction. The convergence in frequently applied methods is not as evident as among the *CHL* algorithms in Fig. 1. The advantage of semi-analytical over empirical algorithms is a matter of adaptivity and justification rather than accuracy. Application of semi-analytical algorithms implies a physically sound procedure with defined R_{rs}^+ from atmospheric correction procedures as mentioned for *CHL* (Moore et al., 1999; Ruddick et al., 2000; Stumpf et al., 2003). Their configuration allows adjustment to other sensors or bands (Van der Woerd & Pasterkamp, 2004), and comparison of atmospheric corrections (Matthews et al., 2010) or reflectance models (Nechad et al., 2010). In contrast, empirical algorithms apart from Petus et al. (2010) and Mélin et al. (2007) are applied to uncorrected at-sensor radiances (Koponen et al., 2007) and physically undefined reflectance quantities (Chen et al., 2009; Wang et al., 2009), leaving them unjustified for applications beyond the data they are derived for. However, empirical algorithms are advantageous for evaluation experiments as with the validation of *TSM* from geostationary MSG-SEVIRI data by means of MODIS *TSM* (Neukermans et al., 2009).

An increase in spectral band position with observed *TSM* concentration range is found in Fig. 2 as well as in several discussions (Fettweis et al., 2011; Wang & Lu, 2010; Zhang et al., 2010). Maximum sensitivity thresholds are estimated at 30 g/m³ g/m³ for SeaWiFS' 555 nm band (Eleveld et al., 2008) or around 150–200 g/m³ for bands at <650 nm (Fettweis et al., 2011; Wang & Lu, 2010). Only one recent quantitative validation experiment investigates such
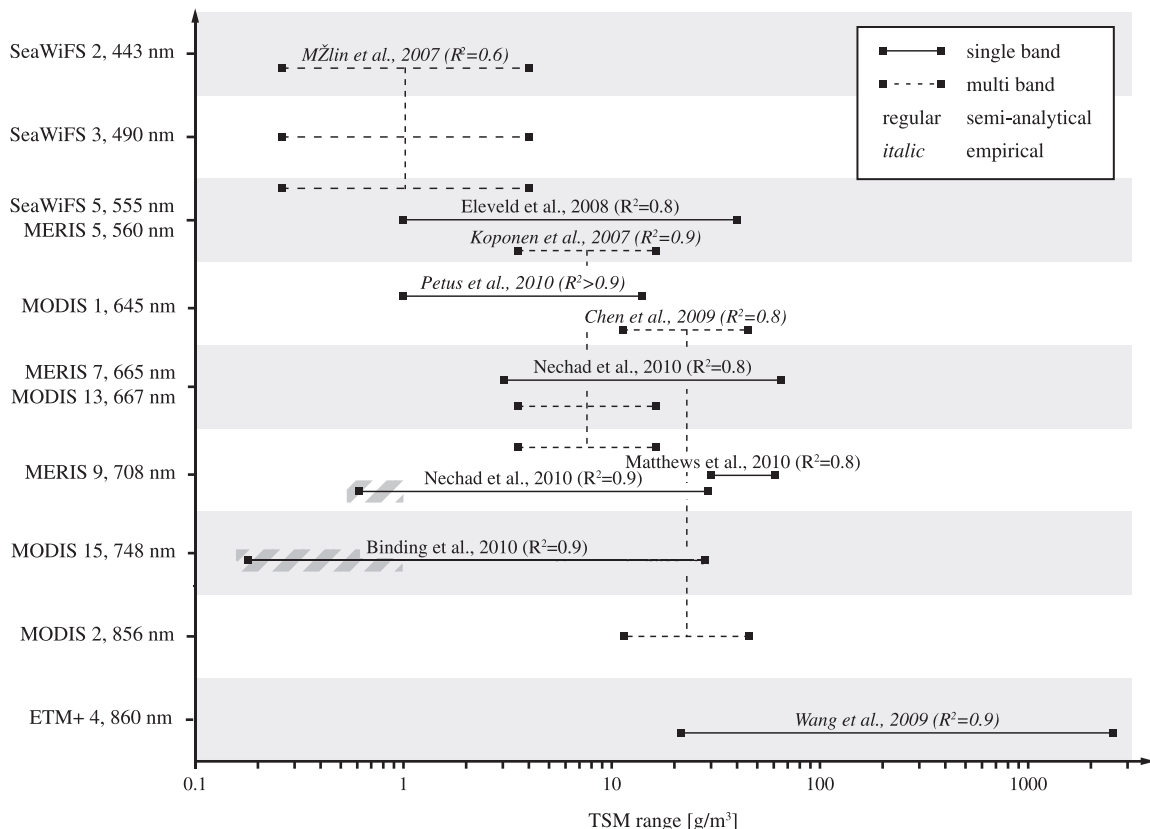

Fig. 2. Overview of recently (2006–2011) published ISI journal papers on the separate retrieval of TSM from satellite imagery by means of matchup-validated semi-analytical and empirical algorithms. Hatched areas indicate disputed application ranges. The retrieval of tripton from MERIS band 10 (754 nm) at R² = 0.3 was omitted (Yang et al., 2011).

extreme turbidity, accordingly at 860 nm (Wang et al., 2009). In less turbid water, the accuracy variations for 8 MERIS bands between 620 and 885 nm are only $R^2 = 0.89$ to 0.93, and lower in absolute values but similar in variation for MODIS (Nechad et al., 2010). Multi band algorithms are recommended for low *TSM* concentrations due to the increasing superimposition by other constituents' optical properties (Nechad et al., 2010). In this regard, Nechad et al. (2010) suggest a 1 g/m^3 minimum threshold for single band algorithms, while Binding et al. (2010) mention that their RMSE increases to 47% of mean concentrations below 5 g/m^3. Matchups in clear Adriatic coastal water, which is in two thirds of all matchups typically oceanic, confirm the challenges in retrieval of low *TSM*, with a relatively low R^2 (Mélin et al., 2007).

6.3. Dissolved organic matter retrieval

All *CDOM* retrieval band arithmetic algorithms in Fig. 3 are from empirical regression (D'Sa & Miller, 2003; Gitelson et al., 1993; Kallio et al., 2001; Kowalczuk et al., 2005), in the case of Yang et al. (2011) by means of bio-optical simulations (Ammenberg et al., 2002). The examples indicate that single band approaches and bands at less than 490 nm are only applicable to extremely high concentrations and correspondingly strong *CDOM* absorption variations as in Zeekoevlei (Matthews et al., 2010). The two best correlations are calculated for band ratios that apply a 442–490 nm band that is sensitive to both *CHL* and *CDOM* variations, and the *CHL*-sensitive 665 nm band of MERIS for normalization (Koponen et al., 2007; Matthews et al., 2010). In both cases no atmospheric correction is applied, although *CDOM* in the Gulf of Finland is already much less abundant than in Zeekovlei.

Ammenberg et al. (2002) uses the 665 nm band to normalize the 560 nm band rather than the 442–490 nm bands, whereas both the interference with *CHL* absorption and the *CDOM* signal are considerably weaker at 560 nm. The correlation of this ratio with intermediate *CDOM* in Lake Dianchi and Lake Kasumigaura remains however relatively low, in spite of the application of a look-up-table retrieved parameterization (Yang et al., 2011). A recent validation exercise with

ALI bands 2 and 3 at similar spectral positions is only qualitative and thus not included in Fig. 3 (Kutser et al., 2009). Earlier studies have however demonstrated the potential of this band combination for mapping *CDOM* in inland waters even at high spatial resolution (Kutser et al., 2005a; Kutser et al., 2005b).

The SeaWiFS and MODIS bands ratios recommended by Kowalczuk et al. (2005) and D'Sa and Miller (2003) omit the red-NIR part of the spectrum as previously found for the band arithmetic retrieval of *CHL* with these two instruments. The former was validated with data of the Baltic Sea from both SeaWiFS and MODIS (the latter not shown in Fig. 3, $R^2 = 0.3$) and outperforms the *CDOM* output from SeaDAS semi-analytical algorithms (Carder et al., 1999; Garver & Siegel, 1997; Maritorena et al., 2002) in all cases (Kowalczuk et al., 2010). A SeaWiFS validation in the Mississippi estuary achieves an even higher correlation at lower concentrations (D'Sa et al., 2006). The two validation exercises are also the seasonally most representative ones given that data matchups from several years and seasons are analyzed.

6.4. Spectral inversion applications

13 or a quarter of the selected publications in 2006–2011 ISI journals refer to spectral inversion algorithms (Table 1), with several papers on new algorithms where validation is only a subchapter (Santini et al., 2010; Schroeder et al., 2007b; Van Der Woerd & Pasterkamp, 2008). The quantitative content is often less detailed than with band arithmetic algorithms, hindering an estimate of their applicability as shown in Table 1.

The MERIS algal_2 product (Doerffer & Schiller, 2007) and *CHL* from C2R and its boreal and eutrophic version (Doerffer & Schiller, 2008a; Koponen et al., 2008) have been applied in several experiments. C2R is successfully validated for low to intermediate concentrations (<16 mg/m^3) (Cui et al., 2010; Minghelli-Roman et al., 2011; Odermatt et al., 2010), while C2R and even its eutrophic water version are found unsuitable for high *CHL* concentrations (Binding et al., 2011; Giardino et al., 2010; Matthews et al., 2010). C2R's *CDOM* is found adequate in a eutrophic lagoon in the Baltic Sea, where concurrent *CHL* is strongly
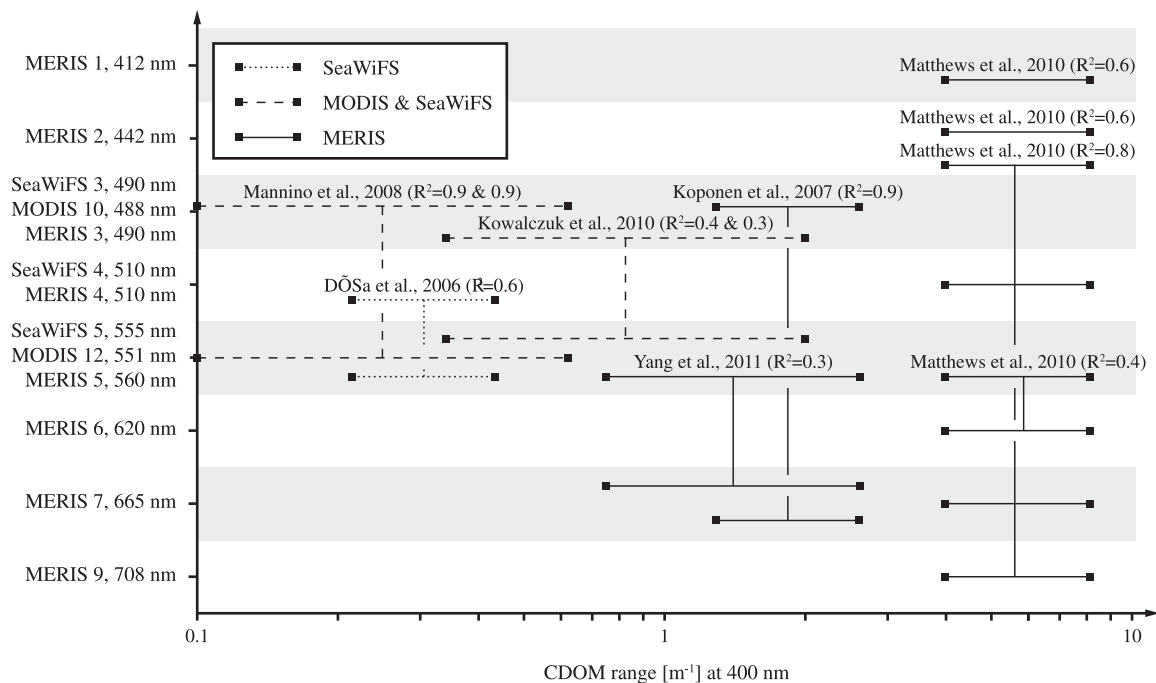
Fig. 3. Overview of recently (2006–2011) published ISI journal papers on the separate retrieval of CDOM from satellite imagery by means of matchup-validated, arithmetic algorithms. Where necessary, normalization to 400 nm is done with explicitly mentioned spectral exponents (Smith & Baker, 1981), i.e. 0.0157 (Yang et al., 2011), 0.0161 (D'Sa et al., 2006) and 0.0188 (Matthews et al., 2010), or an approximate average of 0.0215 (Mannino et al., 2008).

underestimated (Giardino et al., 2010). In contrast, *CDOM* in oligotropic perialpine and Finish lakes is underestimated by both C2R and its boreal version while *CHL* is adequate (Koponen et al., 2008; Odermatt et al., 2010). C2R's atmospheric correction failed at retrieving the red-NIR reflectance peak in several examples, while it outperforms other procedures with its accuracy at blue and green wavelengths (Giardino et al., 2010; Odermatt et al., 2008; Odermatt et al., 2010). *TSM* retrieved by the two NN is inapplicable to turbid water (Cui et al., 2010; Matthews et al., 2010), but accurate at about <15–30 g/m^3 (Koponen et al., 2008).

Validation of the FUB MERIS NN algorithm is successful and thorough at low to intermediate concentrations of all constituents over a wide spatiotemporal range (Schroeder, 2005; Schroeder et al., 2007b). Even lower constituent concentrations are successfully retrieved from a single Hyperion image by means of matrix inversion (Giardino et al., 2007). All other applications do not meet the requirements for quantitative matchup validation. Ground truth comparisons are limited to spectral fits (Van Der Woerd & Pasterkamp, 2008), frequency distribution (Kuchinke et al., 2009b) and transect comparisons (Santini et al., 2010), or display occasional failure that prevent sufficient correlations (Odermatt et al., 2008; Shuchman et al., 2006).

7. Discussion

The assessed quantitative validation experiments using band arithmetic algorithms consist of comparisons of several methods where in situ data are acquired for exactly this validation purpose. They are numerous enough to synthesize several general conclusions based on individual findings and validation sites, e.g. the validity range for red-NIR *CHL* algorithms, the suitability of OC algorithms for low and intermediate *CHL*, the choice of *TSM* retrieval wavelengths according to expected concentrations ranges or the *CHL* variation normalization strategies in *CDOM* retrieval algorithms.

A sufficient number of studies with spectral inversion algorithms are only available for the MERIS NN algorithms. Only the algorithm by Schroeder et al. (2007b) has been successfully validated using matchup correlations of all three constituents over several image acquisitions and aquatic regions as given for many band arithmetic algorithms. We presume two main reasons for this difference, namely availability and complexity. The importance of the availability of algorithms is well represented by the frequent use of retrieval algorithms and corresponding atmospheric correction procedures in SeaDAS and BEAM. They lead to the use of OC algorithms, such as the most popular *CHL* retrieval methods based on SeaWiFS and MODIS data, while NN algorithms are evaluated in most experiments using MERIS data. The opposite cases are rare, although not hindered by sensor or data properties. Consequently, the (semi-)operational use of spectral inversion algorithms is mainly limited to their promoters unless other potential users find easier available methods unsuitable, which may again indicate challenging bio-optical conditions, complicating validation.

Crucial sensor and data properties are the red-NIR wavebands as used in MERIS, the spatial resolution of Landsat and ALI instruments and the temporal resolution of MSG-SEVIRI. In the first case, the red-NIR *CHL* retrieval experiments with MERIS outnumber and outperform corresponding experiments for most other sensors, rendering MERIS the preferred instrument for estimating *CHL* in meso- to eutrophic waters. In the case of MSG-SEVIRI, TM, ETM+ and ALI, radiometric accuracy, bandwidths and a lack of appropriate preprocessing tools complicate routine use, as established with dedicated ocean color instruments. However, experimental evidence is given that either of those instruments can be used for case 2 water constituent retrieval under certain circumstances. Simpler methods are however mostly empirical, providing rapid access to data and their correlations, but at the cost of being site specific and not expressing any cause–effect relationship.

On the opposite side, complexity in constitution, application and validation of spectral inversion procedures are clearly highest. They retrieve several aquatic and possibly atmospheric parameters from a larger number of spectral bands. Failure at any point in the procedure, i.e. the assumption of an inappropriate shape in *CDOM* absorption, may propagate errors in the estimates of other parameters, complicating a coherent validation or falsification. Band arithmetic algorithms on the contrary make use of known relationships between one aquatic parameter and 1–3 spectral bands that are sensitive to an optical property of the sought-after parameter or allow the normalization of other variations. The validation or falsification of such relationships is straightforward and reveals a good estimate of an algorithm's validity range.

For a comparison of the known validity ranges for band arithmetic algorithms (Fig. 1 to Fig. 3), we apply a scheme that helps to further categorize applications for case 2 waters. Natural variations in each constituent are separated in a low, intermediate and high range. Low *CHL* is referred to as oligotrophic, and ranges up to 3 mg/m^3, the integer average from ecological classification schemes (Bukata et al., 1995; Carlson & Simpson, 1996; Chapra & Dobson, 1981; Nürnberg, 1996; Wetzel, 1983). Previous definitions of the second threshold between mesotrophic and eutrophic waters differ from 5.6 to 20 mg/m^3 and are supplemented with a hypereutrophic water in some schemes (Table 2). According to these sources and Fig. 1 we set the threshold to 10 mg/m^3, which approximately limits the applicability of OC and red-NIR algorithms at the top and bottom of their concentration range, respectively. *TSM* thresholds are set at 3 and 30 g/m^3 due to the experimental ranges in Fig. 2, corresponding water types are referred to as clear, cloudy or turbid. An analogous portioning is carried out for *CDOM* according to Fig. 3, allowing the assignment of all collected validation experiments to one or several variation spaces with regard to independent variations in the other two constituents as in Fig. 4 (e.g. *TSM* retrieval in clear and cloudy water at given *CHL* and *CDOM* (Binding et al., 2010)).

Published validation experiments as used in Fig. 1 to Fig. 3 are depicted in Fig. 4 if variation ranges of all three constituents are given, even if only individual constituents are retrieved. Only two spectral inversion experiments from Table 1 can be positioned. Schroeder et al. (2007b) present simultaneous retrieval of all parameters at an accuracy that is comparable to corresponding band-ratio validations, while only *CHL* is retrieved accurately in Cui et al. (2010), but variations in *TSM* and *CDOM* are also given. The *CHL* retrieval column in Fig. 4 shows the suitability of red-NIR algorithms for eutrophic water, and the potential of OC algorithms for oligo- to mesotrophic waters at relatively low *TSM* and *CDOM* variations. Several different algorithms retrieve *TSM* accurately, but the relationship between sensitive wavelength and concentration range (Fig. 2) is no more visible. Relatively few experiments are assigned to turbid water, probably because measuring in situ *TSM* is much less of an effort than additional *CHL* and *CDOM*. The proof of successful *CDOM* retrieval is however generally scarce, similar as with low *CHL* concentrations.

The directional reflectance properties of water are often neglected. Spectral inversion algorithms that make use of directional radiative transfer simulations are the most adequate solution, as they can account for all influencing parameters assuming a given $\tilde{\beta}(\psi)$

Table 2
Trophic levels for coastal and inland waters and corresponding CHL [mg/m^3].

Author	Oligotrophic	Mesotrophic	Eutrophic	Hypereutr.
Chapra and Dobson (1981)	0–2.9	2.9–5.6	>5.6	n.a.
Wetzel (1983)	0.3–4.5	3–11	3–78	n.a.
Bukata et al. (1995)	0.8–2.5	2.5–6	6–18	>18
Carlson and Simpson (1996)	0–2.6	2.6–20	20–56	>56
Nürnberg (1996)	0–3.5	3.5–9	9–25	>25
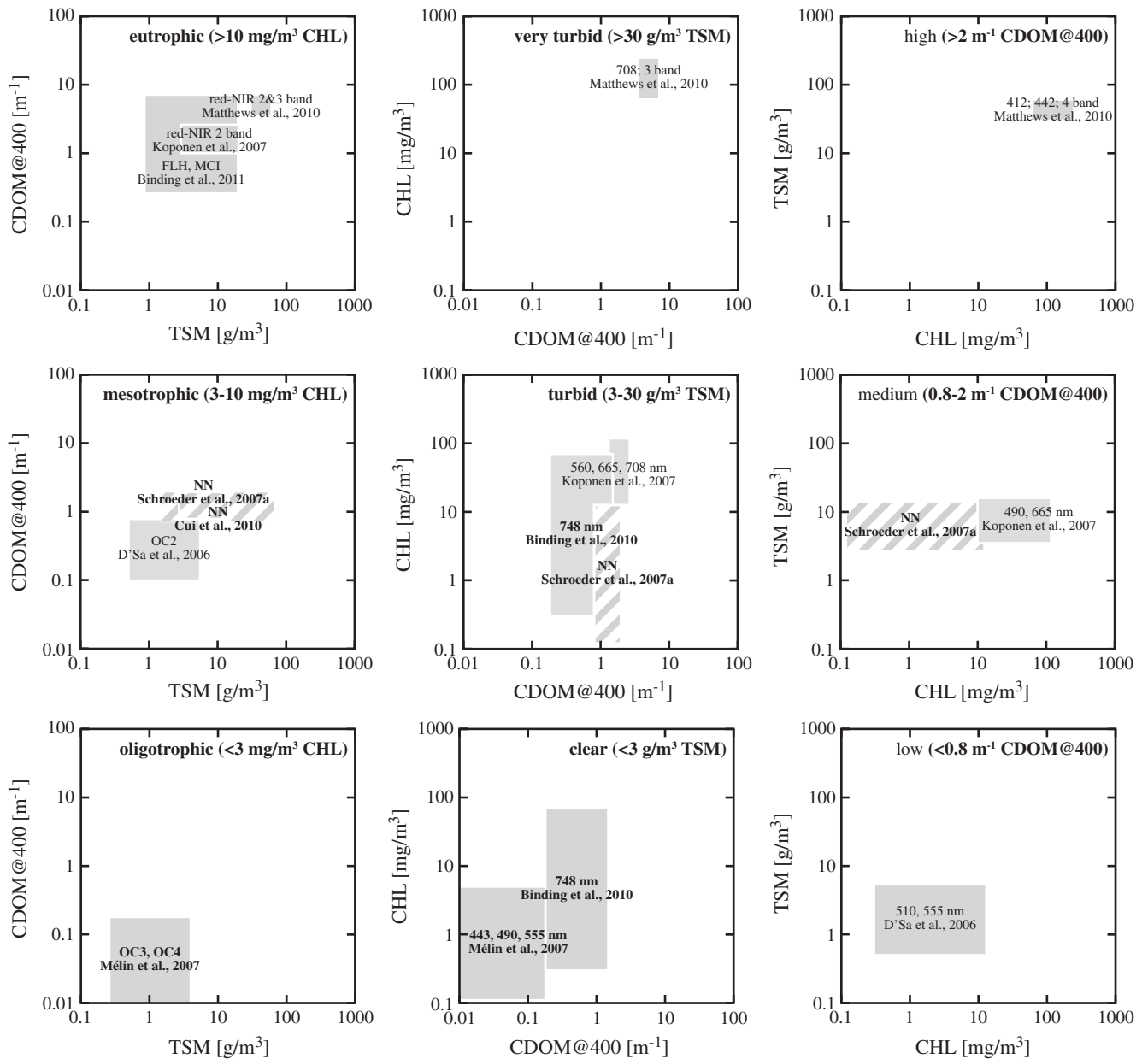
Fig. 4. Case 2 water classes for CHL (left column), TSM (center) and CDOM (right) concentrations, with high to low concentration classes from top to bottom, and the remaining two constituents varying in x- and y-directions of each box. Class names and concentration ranges are titled in each box. Algorithm validation ranges are indicated as boxes and labeled with corresponding retrieval methods or center wavelengths. Bold labels indicate validation experiments with >10 images, hatched areas indicate simultaneous retrieval of all constituents. Reading example: Binding et al. (2011) validate the FLH and MCI algorithms for CHL in eutrophic waters with 0.85–19.60 g/m³ TSM and 0.26-7.14 m⁻¹ CDOM.

(Doerffer & Schiller, 2008a; Giardino et al., 2007; Van Der Woerd & Pasterkamp, 2008). Regarding classical analytical approaches, directional effects are parameterized using coefficients (e.g. f, Q) that vary with constituent concentrations (Morel & Gentili, 1991, 1993). Their estimation requires iterative optimization, which needs an extension for band arithmetic analysis (Yang et al., 2011). More recent analytical models are even parameterized with a specific geometry (Albert & Mobley, 2003; Park & Ruddick, 2005). A corresponding application example is given in Nechad et al. (2010), where the retrieval of *TSM* from cloudy water using a classical model (Gordon et al., 1988) is surprisingly better than a directional model (Park & Ruddick, 2005). Nonetheless, an improvement is expected especially for water with less particle scattering, i.e. higher η and lower N, and thus with higher anisotropy. Atmospheric correction procedures that provide an accurate $[R_w]_N$ e.g. through iterative procedures are

thereby eligible alternatives to more extensively parameterized reflectance models.

The prominence of band-ratio algorithms for the individual retrieval of CHL in case 2 waters reported in this study, warrants however a note of caution. It has been suggested that changes on phytoplankton assemblages, as due to climate change, may shift phytoplankton composition in response to altered environmental forcing (e.g. Montes-Hugo et al., 2008). This process might uncouple *CDOM* and *TSM* concentrations from phytoplankton stocks and lead to further uncertainty in the retrieval of individual constituents, which is usually the case when using empirical algorithms, as opposed to the consolidated retrieval by inversion algorithms (Dierssen, 2010).

Extending from the intercomparison of algorithms performance based on synthetic and in situ data sets (IOCCG, 2006), a series of intercomparison and benchmark exercises including application to

satellite imagery and matchup analysis is recommended to shed light on the comparability of water constituent retrieval algorithms and identify their applicability constraints in the near future.

Acknowledgements

References

Aiken, J., Moore, G. F., Trees, C. C., Hooker, S. B., & Clark, D. K. (1995). The SeaWiFS CZCS-type pigment algorithm. In S. B. Hooker, & E. R. Firestone (Eds.), SeaWiFS Technical Report Series, 29, : Goddard Space Flight Center 38 p.

Albert, A., & Mobley, C. D. (2003). An analytical model for subsurface irradiance and remote sensing reflectance in deep and shallow case-2 water. Optics Express, 11(22), 2873–2890.

Ammenberg, P., Flink, P., Lindell, T., Pierson, D. C., & Strombeck, N. (2002). Bio-optical modelling combined with remote sensing to assess water quality. International Journal of Remote Sensing, 23/8, 1621.

Austin, R. W., & Petzold, T. J. (1981). Water colour measurements. In J. Gower (Ed.), Oceanography from space (pp. 239–256). New York: Plenum.

Babin, M., Stramski, D., Ferrari, G. M., Claustre, H., Bricaud, A., Obolensky, G., & Hoepffner, N. (2003). Variations in the light absorption coefficients of phytoplankton, nonalgal particles, and dissolved organic matter in coastal waters around Europe. Journal of Geophysical Research, 108/C7, 3211.

Belzile, C., Vincent, W. F., Howard-Williams, C., Hawes, I., James, M. R., Kumagai, M., & Roesler, C. S. (2004). Relationships between spectral optical properties and optically active substances in a clear oligotrophic lake. Water Resources Research, 40, W12512.

Binding, C. E., Greenberg, T. A., Jerome, J. H., Bukata, R. P., & Letourneau, G. (2011). An assessment of MERIS algal products during an intense bloom in Lake of the Woods. Journal of Plankton Research, 33(5), 793–806.

Binding, C. E., Jerome, J. H., Bukata, R. P., & Booty, W. G. (2010). Suspended particulate matter in Lake Erie derived from MODIS aquatic colour imagery. International Journal of Remote Sensing, 31(19), 5239–5255.

Brando, V. E., & Dekker, A. G. (2003). Satellite hyperspectral remote sensing for estimating estuarine and coastal water quality. IEEE Transactions on Geoscience and Remote Sensing, 41(6), 1378–1387.

Bricaud, A., Morel, A., & Prieur, L. (1981). Absorption by dissolved organic matter of the sea (yellow substance) in the UV and visible domains. Limnology and Oceanography, 26(1), 43–53.

Bricaud, A., Roesler, C., & Zaneveld, J. R. V. (1995). In situ methods for measuring the inherent optical properties of ocean waters. Limnology and Oceanography, 40(2), 393–410.

Bukata, R. P., Jerome, J. H., Kondratyev, K. Y., & Pozdnyakov, D. V. (1995). Optical properties and remote sensing of inland and coastal waters. USA: CRS Press.

Bulgarelli, B., Kiselev, V., & Roberti, L. (1999). Radiative transfer in the atmosphere–ocean system: The finite-element method. Applied Optics, 38/9, 1530–1542.

Carder, K. L., Chen, F. R., Lee, Z. P., Hawes, S. K., & Kamykowski, D. (1999). Semianalytic Moderate-Resolution Imaging Spectrometer algorithms for chlorophyll a and absorption with bio-optical domains based on nitrate-depletion temperatures. Journal of Geophysical Research, 104/C3, 5403–5421.

Carlson, R. E., & Simpson, J. (1996). A coordinator's guide to volunteer lake monitoring methods. : North American Lake Management Society 96 p.

Chami, M., McKee, D., Leymarie, E., & Khomenko, G. (2006). Influence of the angular shape of the volume-scattering function and multiple scattering on remote sensing reflectance. Applied Optics, 45/36, 9210–9220.

Chapra, S. C., & Dobson, H. F. H. (1981). Quantification of the lake trophic typologies of Naumann (surface quality) and Thienemann (oxygen) with special reference to the great lakes. Journal of Great Lakes Research, 7(2), 182–193.

Chen, S., Fang, L., Li, H., Chen, W., & Huang, W. (2011). Evaluation of a three-band model for estimating chlorophyll-a concentration in tidal reaches of the Pearl River Estuary, China. ISPRS Journal of Photogrammetry and Remote Sensing, 66(3), 356–364.

Chen, S., Huang, W., Wang, H., & Li, D. (2009). Remote sensing assessment of sediment re-suspension during Hurricane Frances in Apalachicola Bay, USA. Remote Sensing of Environment, 113(12), 2670–2681.

Cheng Feng, L., Yun Mei, L., Yong, Z., Deyong, S., & Bin, Y. (2009). Validation of a quasi-analytical algorithm for highly turbid eutrophic water of Meiliang Bay in Taihu Lake, China. IEEE Transactions on Geoscience and Remote Sensing, 47(8), 2492–2500.

Clark, D. (1997). Bio-optical algorithms — Case 1 waters. MODIS algorithm theoretical basis document, Version 1.2. : National Oceanic and Atmospheric Administration 50 p.

Cooley, T., Anderson, G. P., Felde, G. W., Hoke, M. L., Ratkowski, A. J., Chetwynd, J. H., Gardner, J. A., Adler-Golden, S. M., Matthew, M. W., Berk, A., Bernstein, L. S., Acharya, P. K., Miller, D., & Lewis, P. (2002). FLAASH, a Modtran4-based atmospheric correction algorithm, its application and validation. Proc. Geoscience and Remote Sensing Symposium, 2002. IGARSS '02. 2002 IEEE International, vol.1413. (pp. 1414–1418).

Cui, T., Zhang, J., Groom, S., Sun, L., Smyth, T., & Sathyendranath, S. (2010). Validation of MERIS ocean-color products in the Bohai Sea: A case study for turbid coastal waters. Remote Sensing of Environment, 114(10), 2326–2336.

Dall'Olmo, G., & Gitelson, A. A. (2006). Effect of bio-optical parameter variability and uncertainties in reflectance measurements on the remote estimation of chlorophyll-a concentration in turbid productive waters: Modeling results. Applied Optics, 45(15), 3577–3593.

Dall'Olmo, G., Gitelson, A. A., & Rundquist, D. C. (2003). Towards a unified approach for remote estimation of chlorophyll-a in both terrestrial vegetation and turbid productive waters. Geophysical Research Letters, 30/18, 1938.

Dekker, A. G., Malthus, T. J., & Hoogenboom, H. J. (1995). The remote sensing of inland water quality. In F. M. Danson, & S. E. Plummer (Eds.), Advances in environmental remote sensing (pp. 123–142). : John Wiley & Sons Ltd.

Dekker, A. G., & Peters, S. W. M. (1993). Use of the thematic mapper for the analysis of eutrophic lakes: A case study in the Netherlands. International Journal of Remote Sensing, 14(5), 799–821.

Dierssen, H. M. (2010). Perspectives on empirical approaches for ocean color remote sensing of chlorophyll in a changing climate. Proceedings of the National Academy of Sciences, 107(40), 17073–17078.

Doerffer, R., & Schiller, H. (2007). The MERIS case 2 water algorithm. International Journal of Remote Sensing, 28(3), 517–535.

Doerffer, R., & Schiller, H. (2008). MERIS lake water algorithm for BEAM. BEAM algorithm technical basis document. Geesthacht, Germany: GKSS Forschungszentrum 17 p.

Doerffer, R., & Schiller, H. (2008). MERIS regional coastal and lake case 2 water project atmospheric correction. BEAM algorithm technical basis document. Geesthacht, Germany: GKSS Forschungszentrum 42 p.

D'Sa, E. J., & Miller, R. L. (2003). Bio-optical properties in waters influenced by the Mississippi River during low flow conditions. Remote Sensing of Environment, 84/4, 538.

D'Sa, E. J., Miller, R. L., & Del Castillo, C. (2006). Bio-optical properties and ocean color algorithms for coastal waters influenced by the Mississippi River during a cold front. Applied Optics, 45/28, 7410–7428.

Dupouy, C., Neveux, J., Ouillon, S., Frouin, R., Murakami, H., Hochard, S., & Dirberg, G. (2010). Inherent optical property and satellite retrieval of chlorophyll concentration in the lagoon and open ocean waters of New Caledonia. Marine Pollution Bulletin, 61(7–12), 503–518.

Eleveld, M. A., Pasterkamp, R., van der Woerd, H. J., & Pietrzak, J. D. (2008). Remotely sensed seasonality in the spatial distribution of sea-surface suspended particulate matter in the southern North Sea. Estuarine, Coastal and Shelf Science, 80(1), 103–113.

Ferreira, A. B., Garcia, V. M. T., & Garcia, C. A. E. (2009). Light absorption by phytoplankton, non-algal particles and dissolved organic matter at the Patagonia shelf-break in spring and summer. Deep Sea Research Part I: Oceanographic Research Papers, 56/12, 2162–2174.

Fettweis, M., Baeye, M., Francken, F., Lauwaert, B., Van den Eynde, D., Van Lancker, V., Martens, C., & Michielsen, T. (2011). Monitoring the effects of disposal of fine sediments from maintenance dredging on suspended particulate matter concentration in the Belgian nearshore area (southern North Sea). Marine Pollution Bulletin, 62(2), 258–269.

Fournier, G. R., & Forand, J. L. (1994). Analytic phase function for ocean water. Norway: Bergen.

Fournier, G. R., & Jonasz, M. (1999). Computer-based underwater imaging analysis. USA: Denver, CO.

Freda, W., Król, T., Martynov, O. V., Shybanov, E. B., & Hapter, R. (2007). Measurements of scattering function of sea water in Southern Baltic. The European Physical Journal — Special Topics, 144(1), 147–154.

Freda, W., & Piskozub, J. (2007). Improved method of Fournier–Forand marine phase function parameterization. Optics Express, 15(20), 12763–12768.

Garver, S. A., & Siegel, D. A. (1997). Inherent optical property inversion of ocean color spectra and its biogeochemical interpretation 1. Time series from the Sargasso Sea. Journal of Geophysical Research, 102/C8, 18607–18625.

Giardino, C., Brando, V. E., Dekker, A. G., Strömbeck, N., & Candiani, G. (2007). Assessment of water quality in Lake Garda (Italy) using Hyperion. Remote Sensing of Environment, 109(2), 183–195.

Giardino, C., Bresciani, M., Pilkaityte, R., Bartoli, M., & Razinkovas, A. (2010). In situ measurements and satellite remote sensing of case 2 waters: First results from the Curonian Lagoon. Oceanologia, 52(2), 197–210.

Gitelson, A. (1992). The peak near 700 nm on radiance spectra of algae and water: Relationships of its magnitude and position with chlorophyll concentration. International Journal of Remote Sensing, 13(17), 3367–3373.

Gitelson, A. A., Dall'Olmo, G., Moses, W., Rundquist, D. C., Barrow, T., Fisher, T. R., Gurlin, D., & Holz, J. (2008). A simple semi-analytical model for remote estimation of chlorophyll-a in turbid waters: Validation. Remote Sensing of Environment, 112(9), 3582–3593.

Gitelson, A., Gao, B. -C., Li, R. -R., Berdnikov, S., & Saprygin, V. (2011). Estimation of chlorophyll-a concentration in productive turbid waters using a Hyperspectral Imager for the Coastal Ocean: The Azov Sea case study. Environmental Research Letters, 6/024023, 6.

Gitelson, A., Garbuzov, G., Szilagyi, F., Mittenzwey, K. H., Karnieli, A., & Kaiser, A. (1993). Quantitative remote sensing methods for real-time monitoring of inland waters quality. International Journal of Remote Sensing, 14(7), 1269–1295.

Gitelson, A., Gurlin, D., Moses, W. J., & Barrow, T. (2009). A bio-optical algorithm for the remote estimation of the chlorophyll-a concentration in case 2 waters. Environmental Research Letters, 4/045003, 5.

Gitelson, A. A., Schalles, J. F., & Hladik, C. M. (2007). Remote chlorophyll-a retrieval in turbid, productive estuaries: Chesapeake Bay case study. *Remote Sensing of Environment*, 109(4), 464–472.

Gons, H. J., Auer, M. T., & Effler, S. W. (2008). MERIS satellite chlorophyll mapping of oligotrophic and eutrophic waters in the Laurentian Great Lakes. *Remote Sensing of Environment*, 112(11), 4098–4106.

Gonzalez Vilas, L., Spyrakos, E., & Torres Palenzuela, J. M. (2011). Neural network estimation of chlorophyll a from MERIS full resolution data for the coastal waters of Galician rias (NW Spain). *Remote Sensing of Environment*, 115(2), 524–535.

Gordon, H. R. (1989). Dependence of the diffuse reflectance of natural waters on the sun angle. *Limnology and Oceanography*, 34(8), 1484–1489.

Gordon, H. R. (1993). Sensitivity of radiative transfer to small-angle scattering in the ocean: Quantitative assessment. *Applied Optics*, 32(36), 7505–7511.

Gordon, H. R., & Brown, O. B. (1973). Irradiance reflectivity of a flat ocean as a function of its optical properties. *Applied Optics*, 12/7, 1549–1551.

Gordon, H. R., Brown, O. B., Evans, R. H., Brown, J. W., Smith, R. C., Baker, K. S., & Clark, D.K. (1988). A semianalytic radiance model of ocean color. *Journal of Geophysical Research*, 93/D9, 10909–10924.

Gordon, H. R., Brown, O. B., & Jacobs, M. M. (1975). Computed relationships between the inherent and apparent optical properties of a flat homogeneous ocean. *Applied Optics*, 14/2, 417–427.

Gordon, H. R., & Clark, D. K. (1981). Clear water radiances for atmospheric correction of coastal zone color scanner imagery. *Applied Optics*, 20/24, 4175–4180.

Gordon, H. R., & Franz, B. A. (2008). Remote sensing of ocean color: Assessment of the water-leaving radiance bidirectional effects on the atmospheric diffuse transmittance for SeaWiFS and MODIS intercomparisons. *Remote Sensing of Environment*, 112(5), 2677–2685.

Gordon, H. R., & Voss, K. J. (2004). MODIS normalized water-leaving radiance. *MODIS algorithm theoretical basis documents, MOD-18* 125 p.

Gordon, H. R., & Wang, M. (1994). Retrieval of water-leaving radiance and aerosol optical thickness over the oceans with SeaWiFS: A preliminary algorithm. *Applied Optics*, 33, 443–452.

Gower, J. F. R., Doerffer, R., & Borstad, G. A. (1999). Interpretation of the 685nm peak in water-leaving radiance spectra in terms of fluorescence, absorption and scattering, and its observation by MERIS. *International Journal of Remote Sensing*, 20(9), 1771–1786.

Gower, J., King, S., Borstad, G., & Brown, L. (2005). Detection of intense plankton blooms using the 709 nm band of the MERIS imaging spectrometer. *International Journal of Remote Sensing*, 26/9.

Guanter, L., Ruiz-Verdu, A., Odermatt, D., Giardino, C., Simis, S., Estelles, V., Heege, T., Dominguez-Gomez, J. A., & Moreno, J. (2010). Atmospheric correction of ENVISAT/-MERIS data over inland waters: Validation for European lakes. *Remote Sensing of Environment*, 114(3), 467–480.

Haltrin, V. I. (2002). One-parameter two-term henyey-greenstein phase function for light scattering in seawater. *Applied Optics*, 41/6, 1022–1028.

Heege, T., & Fischer, J. (2004). Mapping of water constituents in Lake Constance using multispectral airborne scanner data and a physically based processing scheme. *Canadian Journal of Remote Sensing*, 30(1), 77–86.

Horion, S., Bergamino, N., Stenuite, S., Descy, J. P., Plisnier, P. D., Loiselle, S. A., & Cornet, Y. (2010). Optimized extraction of daily bio-optical time series derived from MODIS/Aqua imagery for Lake Tanganyika, Africa. *Remote Sensing of Environment*, 114(4), 781–791.

Hu, C., Carder, K. L., & Muller-Karger, F. E. (2000). Atmospheric correction of SeaWiFS imagery over turbid coastal waters: A practical method. *Remote Sensing of Environment*, 74/2, 195.

Iluz, D., Yacobi, Y. Z., & Gitelson, A. A. (2003). Adaptation of an algorithm for chlorophyll-a estimation by optical data in the oligotrophic Gulf of Eilat. *International Journal of Remote Sensing*, 24/5, 1157.

IOCCG (2006). Remote sensing of inherent optical properties: Fundamentals, tests of algorithms, and applications. In Z. P. Lee (Ed.), *Reports of the International Ocean-Colour Coordinating Group*: IOCCG 122 p.

IOCCG, & Partition of the Ocean into Ecological Provinces: Role of Ocean-Colour Radiometry (2009). In M. Dowell, & T. Platt (Eds.), *Reports of the International Ocean-Colour Coordinating Group*. : IOCCG 98 p.

Jerome, J. H., Bukata, R. P., & Miller, J. R. (1996). Remote sensing reflectance and its relationship to optical properties of natural waters. *International Journal of Remote Sensing*, 17(16), 3135–3155.

Jin, Z., & Stamnes, K. (1994). Radiative transfer in nonuniformly refracting layered media: Atmosphere–ocean system. *Applied Optics*, 33, 431–442.

Kabbara, N., Benkhelil, J., Awad, M., & Barale, V. (2008). Monitoring water quality in the coastal area of Tripoli (Lebanon) using high-resolution satellite data. *ISPRS Journal of Photogrammetry and Remote Sensing*, 63(5), 488–495.

Kallio, K., Kutser, T., Hannonen, T., Koponen, S., Pulliainen, J., Vepsalainen, J., & Pyhalahti, T. (2001). Retrieval of water quality from airborne imaging spectrometry of various lake types in different seasons. *The Science of the Total Environment*, 268(1–3), 59–77.

Kirk, J. T. O. (1991). Volume scattering function, average cosines, and the underwater light field. *Limnology and Oceanography*, 36(3), 455–467.

Koponen, S., Attila, J., Pulliainen, J., Kallio, K., Pyh‰lahti, T., Lindfors, A., Rasmus, K., & Hallikainen, M. (2007). A case study of airborne and satellite remote sensing of a spring bloom event in the Gulf of Finland. *Continental Shelf Research*, 27/2, 228–244.

Koponen, S., Ruiz-Verdu, A., Heege, T., Heblinski, J., Sorensen, K., Kallio, K., Pyhalahti, T., Doerffer, R., Brockmann, C., & Peters, M. (2008). Development of MERIS lake water algorithms. *ESA Validation Report* 65 p.

Kostadinov, T. S., Siegel, D. A., Maritorena, S., & Guillocheau, N. (2007). Ocean color observations and modeling for an optically complex site: Santa Barbara Channel, California, USA. *Journal of Geophysical Research*, 112/C7, C07011.

Kowalczuk, P., Darecki, M., Zablocka, M., & Gorecka, I. (2010). Validation of empirical and semi-analytical remote sensing algorithms for estimating absorption by coloured dissolved organic matter in the Baltic Sea from SeaWiFS and MODIS imagery. *Oceanologia*, 52(2), 171–196.

Kowalczuk, P., Olszewski, J., Darecki, M., & Kaczmarek, S. (2005). Empirical relationships between coloured dissolved organic matter (CDOM) absorption and apparent optical properties in Baltic Sea waters. *International Journal of Remote Sensing*, 26(2), 345–370.

Kuchinke, C. P., Gordon, H. R., & Franz, B. A. (2009). Spectral optimization for constituent retrieval in Case 2 waters I: Implementation and performance. *Remote Sensing of Environment*, 113(3), 571–587.

Kuchinke, C. P., Gordon, H. R., Harding, L. W., Jr., & Voss, K. J. (2009). Spectral optimization for constituent retrieval in Case 2 waters II: Validation study in the Chesapeake Bay. *Remote Sensing of Environment*, 113(3), 610–621.

Kutser, T., Herlevi, A., Kallio, K., & Arst, H. (2001). A hyperspectral model for interpretation of passive optical remote sensing data from turbid lakes. *The Science of the Total Environment*, 268/1-3, 47.

Kutser, T., Paavel, B., Metsamaa, L., & Vahtmäe, E. (2009). Mapping coloured dissolved organic matter concentration in coastal waters. *International Journal of Remote Sensing*, 30(22), 5843–5849.

Kutser, T., Pierson, D. C., Kallio, K. Y., Reinart, A., & Sobek, S. (2005). Mapping lake CDOM by satellite remote sensing. *Remote Sensing of Environment*, 94/4, 535.

Kutser, T., Pierson, D. C., Tranvik, L., Reinart, A., Sobek, S., & Kallio, K. Y. (2005). Using satellite remote sensing to estimate the colored dissolved organic matter absorption coefficient in lakes. *Ecosystems*, 8/6, 709.

Lee, Z., Carder, K. L., & Arnone, R. A. (2002). Deriving inherent optical properties from water color: A multiband quasi-analytical algorithm for optically deep waters. *Applied Optics*, 41/27, 5755–5772.

Lee, Z., Carder, K. L., Mobley, C. D., Steward, R. G., & Patch, J. S. (1998). Hyperspectral remote sensing for shallow waters. I. A Semianalytical model. *Applied Optics*, 37/27, 6329–6338.

Lee, M. E., & Lewis, M. R. (2003). A new method for the measurement of the optical volume scattering function in the upper ocean. *Journal of Atmospheric and Oceanic Technology*, 20(4), 563–571.

Loisel, H., & Morel, A. (2001). Non-isotropy of the upward radiance field in typical coastal (Case 2) waters. *International Journal of Remote Sensing*, 22(2), 275–295.

Mahasandana, S., Tripathi, N. K., & Honda, K. (2009). Sea surface multispectral index model for estimating chlorophyll a concentration of productive coastal waters in Thailand. *Canadian Journal of Remote Sensing*, 35(3), 287–296.

Mannino, A., Russ, M. E., & Hooker, S. B. (2008). Algorithm development and validation for satellite-derived distributions of DOC and CDOM in the U.S. Middle Atlantic Bight. *J. Geophys. Res.*, 113/C7, C07051.

Maritorena, S., Siegel, D. A., & Peterson, A. R. (2002). Optimization of a semianalytical ocean color model for global-scale applications. *Applied Optics*, 41/15, 2705–2714.

Matthews, M. W. (2011). A current review of empirical procedures of remote sensing in inland and near-coastal transitional waters. *International Journal of Remote Sensing*, 32(21), 6855–6899.

Matthews, M. W., Bernard, S., & Winter, K. (2010). Remote sensing of cyanobacteria-dominant algal blooms and water quality parameters in Zeekoevlei, a small hypertrophic lake, using MERIS. *Remote Sensing of Environment*, 114(9), 2070–2087.

McClain, C. R. (2009). A decade of satellite ocean color observations. *Annual Review of Marine Science*, 1(1), 19–42.

Mélin, F., Zibordi, G., & Berthon, J. -F. (2007). Assessment of satellite ocean color products at a coastal site. *Remote Sensing of Environment*, 110(2), 192–215.

Minghelli-Roman, A., Laugier, T., Polidori, L., Mathieu, S., Loubersac, L., & Gouton, P. (2011). Satellite survey of seasonal trophic status and occasional anoxic 'malaigue' crises in the Thau lagoon using MERIS images. *International Journal of Remote Sensing*, 32(4), 909–923.

Mobley, C. D. (1989). A numerical model for the computation of radiance distributions in natural waters with wind-roughened surfaces. *Limnology and Oceanography*, 34(8), 1473–1483.

Mobley, C. D., Gentili, B., Gordon, H. R., Jin, Z., Kattawar, G. W., Morel, A., Reinersman, P., Stamnes, K., & Stavn, R. H. (1993). Comparison of numerical models for computing underwater light fields. *Applied Optics*, 32/36, 7484–7504.

Mobley, C. D., Sundman, L. K., & Boss, E. (2002). Phase function effects on oceanic light fields. *Applied Optics*, 41/6, 1035–1050.

Montes-Hugo, M. A., Vernet, M., Smith, R., & Carder, K. (2008). Phytoplankton size-structure on the western shelf of the Antarctic Peninsula: A remote-sensing approach. *International Journal of Remote Sensing*, 29/3, 801–829.

Moore, G. F., Aiken, J., & Lavender, S. J. (1999). The atmospheric correction of water colour and the quantitative retrieval of suspended particulate matter in Case II waters: Application to MERIS. *International Journal of Remote Sensing*, 20(9), 1713–1733.

Moore, T. S., Campbell, J. W., & Dowell, M. D. (2009). A class-based approach to characterizing and mapping the uncertainty of the MODIS ocean chlorophyll product. *Remote Sensing of Environment*, 113(11), 2424–2430.

Morel, A. (1974). Optical properties of pure water and pure sea water. In N. G. Jerlov, & E. S. Nielsen (Eds.), *Optical aspects of oceanography* (pp. 1–24). New York: Academic Press.

Morel, A. (1980). In-water and remote measurements of ocean color. *Boundary-Layer Meteorology*, 18(2), 177–201.

Morel, A., & Antoine, D. (2007). Pigment index retrieval in case 1 waters. : Laboratoire d'Océanographie de Villefranche 25 p.

Morel, A., Antoine, D., & Gentili, B. (2002). Bidirectional reflectance of oceanic waters: Accounting for Raman emission and varying particle scattering phase function. *Applied Optics*, 41/30, 6289–6306.

Morel, A., & Gentili, B. (1991). Diffuse reflectance of oceanic waters: Its dependence on sun angle as influenced by the molecular scattering contribution. *Applied Optics*, *30/30*, 4427–4438.

Morel, A., & Gentili, B. (1993). Diffuse reflectance of oceanic waters. II Bidirectional aspects. *Applied Optics*, *32/33*, 6864–6879.

Morel, A., & Gentili, B. (1996). Diffuse reflectance of oceanic waters. III. Implication of bidirectionality for the remote-sensing problem. *Appl. Opt.*, 35/24, 4850–4862.

Morel, A., & Maritorena, S. (2001). Bio-optical properties of oceanic waters: A reappraisal. *Journal of Geophysical Research*, *106/C4*, 7163–7180.

Morel, A., & Prieur, L. (1977). Analysis of variations in ocean color. *Limnology and Oceanography*, *22*(4), 709–722.

Moses, W. J., Gitelson, A. A., Berdnikov, S., & Povazhnyy, V. (2009). Estimation of chlorophyll-a concentration in case II waters using MODIS and MERIS data — Successes and challenges. *Environmental Research Letters*, *4/4*, 045005.

Moses, W. J., Gitelson, A. A., Berdnikov, S., & Povazhnyy, V. (2009). Satellite estimation of chlorophyll-a concentration using the red and NIR bands of MERIS — The Azov sea case study. *Geoscience and Remote Sensing Letters, IEEE*, *6/4*, 845–849.

Murakami, H., Sasaoka, K., Hosoda, K., Fukushima, H., Toratani, M., Frouin, R., Mitchell, B., Kahru, M., Deschamps, P. -Y., Clark, D., Flora, S., Kishino, M., Saitoh, S. -I., Asanuma, I., Tanaka, A., Sasaki, H., Yokouchi, K., Kiyomoto, Y., Saito, H., Dupouy, C., Siripong, A., Matsumura, S., & Ishizaka, J. (2006). Validation of ADEOS-II GLI ocean color products using in situ observations. *Journal of Oceanography*, *62*(3), 373–393.

Nechad, B., Ruddick, K. G., & Park, Y. (2010). Calibration and validation of a generic multisensor algorithm for mapping of total suspended matter in turbid waters. *Remote Sensing of Environment*, *114*(4), 854–866.

Neukermans, G., Ruddick, K., Bernard, E., Ramon, D., Nechad, B., & Deschamps, P. -Y. (2009). Mapping total suspended matter from geostationary satellites: A feasibility study with SEVIRI in the Southern North Sea. *Optics Express*, *17*(16), 14029–14052.

Nürnberg, G. K. (1996). Trophic state of clear and colored, soft- and hardwater lakes with special consideration of nutrients, anoxia, phytoplankton and fish. *Lake and Reservoir Management*, *12*(4), 432–447.

Odermatt, D., Giardino, C., & Heege, T. (2010). Chlorophyll retrieval with MERIS Case-2-Regional in perialpine lakes. *Remote Sensing of Environment*, *114*(3), 607–617.

Odermatt, D., Heege, T., Nieke, J., Kneubuehler, M., & Itten, K. (2008). Water quality monitoring for Lake Constance with a physically based algorithm for MERIS data. *Sensors*, *8*(8), 4582–4599.

O'Reilly, J. E., Maritorena, S., Mitchell, B. G., Siegel, D. A., Carder, K. L., Garver, S. A., Kahru, M., & McClain, C. (1998). Ocean color chlorophyll algorithms for SeaWiFS. *Journal of Geophysical Research*, *103/C11*, 24937–24953.

Park, Y., & Ruddick, K. (2005). Model of remote-sensing reflectance including bidirectional effects for case 1 and case 2 waters. *Applied Optics*, *44/7*, 1236–1249.

Petus, C., Chust, G., Gohin, F., Doxaran, D., Froidefond, J. -M., & Sagarminaga, Y. (2010). Estimating turbidity and total suspended matter in the Adour River plume (South Bay of Biscay) using MODIS 250-m imagery. *Continental Shelf Research*, *30*(5), 379–392.

Petzold, T. J. (1972). Volume scattering functions for selected ocean waters. *SIO Ref. 72–78*. Univ. of Calif., San Diego: Scripps Institution of Oceanography 79 p.

Pfeiffer, N., & Chapman, G. H. (2008). Successive order, multiple scattering of two-term Henyey-Greenstein phase functions. *Opt. Express*, *16*(18), 13637–13642.

Piskozub, J., & McKee, D. (2011). Effective scattering phase functions for the multiple scattering regime. *Optics Express*, *19/5*, 4786–4794.

Pozdnyakov, D. V., Shuchman, R., Korosov, A., & Hatt, C. (2005). Operational algorithm for the retrieval of water quality in the Great Lakes. *Remote Sensing of Environment*, *97/3*, 352.

Preisendorfer, R. W. (1961). Application of Radiative Transfer Theory to Light Measurements in the Sea. : International Union of Geodesy and Geophysics Monograph.

Qin, Y., Brando, V. E., Dekker, A. G., & Blondeau-Patissier, D. (2007). Validity of SeaDAS water constituents retrieval algorithms in Australian tropical coastal waters. *Geophysical Research Letters*, *34/21*, L21603.

Ruddick, K. G., De Cauwer, V., Park, Y. -J., & Moore, G. (2006). Seaborne measurements of near infrared water-leaving reflectance: The similarity spectrum for turbid waters. *Limnology and Oceanography*, *51*(2), 1167–1179.

Ruddick, K., Ovidio, F., & Rijkeboer, M. (2000). Atmospheric correction of SeaWiFS imagery for turbid coastal and inland waters. *Applied Optics*, *39*(6), 897–912.

Santini, F., Alberotanza, L., Cavalli, R. M., & Pignatti, S. (2010). A two-step optimization procedure for assessing water constituent concentrations by hyperspectral remote sensing techniques: An application to the highly turbid Venice lagoon waters. *Remote Sensing of Environment*, *114*(4), 887–898.

Sathyendranath, S., & Platt, T. (1997). Analytic model of ocean color. *Applied Optics*, *36/12*, 2620–2629.

Schalles, J. F., Gitelson, A. A., Yacobi, Y. Z., & Kroenke, A. E. (1998). Estimation of chlorophyll-a from time series measurements of high spectral resolution reflectance in an eutrophic lake. *Journal of Phycology*, *34*(2), 383–390.

Schroeder, T. (2005). Fernerkundung von Wasserinhaltsstoffen in Küstengewässern mit MERIS unter Anwendung expliziter und impliziter Atmosphärenkorrekturverfahren. Freie Universität Berlin: Doctoral thesis (in German)

Schroeder, T., Behnert, I., Schaale, M., Fischer, J., & Doerffer, R. (2007). Atmospheric correction algorithm for MERIS above case-2 waters. *International Journal of Remote Sensing*, *28*(7), 1469–1486.

Schroeder, T., Schaale, M., & Fischer, J. (2007). Retrieval of atmospheric and oceanic properties from MERIS measurements: A new Case-2 water processor for BEAM. *International Journal of Remote Sensing*, *28*(24), 5627–5632.

Schuchman, R. A., Korosov, A. A., Pozdnyakov, D. V., Means, J. C., Savage, S., Hatt, C., & Meadows, G. A. (2005). SeaWiFS and MODIS-observed multi-year seasonal and

spatial dynamics in biotic and abiotic processes in Lake Michigan as obtained from a new water quality retrieval algorithm. *Proc. Proc. of 31st Int. Symp. on Remote Sensing of Environment, St. Petersburg, Russia*.

Shanmugam, P., Ahn, Y. -H., Ryu, J. -H., & Sundarabalan, B. (2010). An evaluation of inversion models for retrieval of inherent optical properties from ocean color in coastal and open sea waters around Korea. *Journal of Oceanography*, *66*(6), 815–830.

Shuchman, R., Korosov, A., Hatt, C., Pozdnyakov, D., Means, J., & Meadows, G. (2006). Verification and application of a bio-optical algorithm for Lake Michigan using SeaWiFS: A 7-year inter-annual analysis. *Journal of Great Lakes Research*, *32*(2), 258–279.

Siegel, D. A., Wang, M., Maritorena, S., & Robinson, W. (2000). Atmospheric correction of satellite ocean color imagery: The black pixel assumption. *Applied Optics*, *39*(21), 3582–3591.

Smith, R. C., & Baker, K. S. (1981). Optical properties of the clearest natural waters (200–800 nm). *Applied Optics*, *20*, 177.

Sokolov, A., Chami, M., Dmitriev, E., & Khomenko, G. (2010). Parameterization of volume scattering function of coastal waters based on the statistical approach. *Optics Express*, *18*(5), 4615–4636.

Stumpf, R. P., Arnone, R. A., Gould, R. W., Martinolich, P. M., & Ransibrahmanakul, V. (2003). A partially coupled ocean–atmosphere model for retrieval of water-leaving radiance from SeaWiFS in coastal waters. In S. B. Hooker, & E. R. Firestone (Eds.), *SeaWiFS Postlaunch Tech. Rep. Ser*, *22*, : NASA Goddard Space Flight Cent 51–59 p.

Sullivan, J. M., & Twardowski, M. S. (2009). Angular shape of the oceanic particulate volume scattering function in the backward direction. *Applied Optics*, *48/35*, 6811–6819.

Sydor, M. (2007). Statistical treatment of remote sensing reflectance from coastal ocean water: proportionality of reflectance from multiple scattering to source function b/a. *Journal of Coastal Research*, 1183–1192.

Toratani, M., Fukushima, H., Murakami, H., & Tanaka, A. (2007). Atmospheric correction scheme for GLI with absorptive aerosol correction. *Journal of Oceanography*, *63*(3), 525–532.

Tyler, A. N., Svab, E., Preston, T., Présing, M., & Kovács, A. (2006). Remote sensing of the water quality of shallow lakes: A mixture modelling approach to quantifying phytoplankton in water characterized by high-suspended sediment. *International Journal of Remote Sensing*, *27/8*, 1521.

Van der Woerd, H., & Pasterkamp, R. (2004). Mapping of the North Sea turbid coastal waters using SeaWiFS data. *Canadian Journal of Remote Sensing*, *30*(1), 44–53.

Van Der Woerd, H. J., & Pasterkamp, R. (2008). HYDROPT: A fast and flexible method to retrieve chlorophyll-a from multispectral satellite observations of optically complex coastal waters. *Remote Sensing of Environment*, *112*(4), 1795–1807.

Vasilkov, A., & Kopelevich, O. (1982). The reasons of maximum at about 700 nm on radiance spectra of the sea. *Oceanology*, *22*, 945–950.

Vidot, J., & Santer, R. (2005). Atmospheric correction for inland waters — Application to SeaWiFS. *International Journal of Remote Sensing*, *26/17*, 3663.

Vos, W. L., Donze, M., & Buiteveld, H. (1986). On the reflectance spectrum of algae in water: The nature of the peak at 700 nm and its shift with varying concentration. *Communication on Sanitary Engineering and Water Management* 86–122 p.

Wang, M. (2007). Remote sensing of the ocean contributions from ultraviolet to near-infrared using the shortwave infrared bands: Simulations. *Applied Optics*, *46/9*, 1535–1547.

Wang, J. J., & Lu, X. X. (2010). Estimation of suspended sediment concentrations using Terra MODIS: An example from the Lower Yangtze River, China. *Science of the Total Environment*, *408*(5), 1131–1138.

Wang, J. -J., Lu, X. X., Liew, S. C., & Zhou, Y. (2009). Retrieval of suspended sediment concentrations in large turbid rivers using Landsat ETM+: An example from the Yangtze River, China. *Earth Surface Processes and Landforms*, *34*(8), 1082–1092.

Wang, M., Shi, W., & Tang, J. (2011). Water property monitoring and assessment for China's inland Lake Taihu from MODIS-Aqua measurements. *Remote Sensing of Environment*, *115*(3), 841–854.

Werdell, P. J., Bailey, S. W., Franz, B. A., Harding, L. W., Jr., Feldman, G. C., & McClain, C. R. (2009). Regional and seasonal variability of chlorophyll-a in Chesapeake Bay as observed by SeaWiFS and MODIS-Aqua. *Remote Sensing of Environment*, *113*(6), 1319–1330.

Wetzel, R. G. (1983). *Limnology*. Philadelphia: W.B. Saunders Co.

Witter, D. L., Ortiz, J. D., Palm, S., Heath, R. T., & Budd, J. W. (2009). Assessing the application of SeaWiFS ocean color algorithms to Lake Erie. *Journal of Great Lakes Research*, *35*(3), 361–370.

Yang, W., Matsushita, B., Chen, J., & Fukushima, T. (2011). Estimating constituent concentrations in case II waters from MERIS satellite data by semi-analytical model optimizing and look-up tables. *Remote Sensing of Environment*, *115*(5), 1247–1259.

Zhai, P. -W., Hu, Y., Chowdhary, J., Trepte, C. R., Lucker, P. L., & Josset, D. B. (2010). A vector radiative transfer model for coupled atmosphere and ocean systems with a rough interface. *Journal of Quantitative Spectroscopy and Radiative Transfer*, *111*(7–8), 1025–1040.

Zhang, M., Tang, J., Dong, Q., Song, Q., & Ding, J. (2010). Retrieval of total suspended matter concentration in the Yellow and East China Seas from MODIS imagery. *Remote Sensing of Environment*, *114*(2), 392–403.

Zhou, W., Wang, S., Zhou, Y., & Troy, A. (2006). Mapping the concentrations of total suspended matter in Lake Taihu, China, using Landsat-5 TM data. *International Journal of Remote Sensing*, *27*(6), 1177–1191.